ORNL/SPR-2024/3611

FY24 Milestone M3RD-24OR060404 Measure the effect of molten halide salt exposure on creep rupture lifetime

R. Pillai
B.A. Pint

Approved for public release.
Distribution is unlimited.

September 2024

ORNL IS MANAGED BY UT-BATTELLE LLC FOR THE US DEPARTMENT OF ENERGY

Milestone M3RD-24OR060404
Measure the effect of molten halide salt exposure on creep rupture lifetime
Oak Ridge National Laboratory, Oak Ridge, TN, 37831

Introduction

Recent resurgence in the research and commercial interests in molten salt reactors (MSRs) as a viable advanced reactor concept to achieve the short- and long-term climate goals [1, 2] has resulted in ongoing efforts to demonstrate their commercial potential [3, 4]. These are relying on a combination of the extensive legacy knowledge from the molten salt reactor experiment (MSRE) [5] and relatively recent data on materials compatibility of structural materials of interest such as 316H in molten salts environments [6]. However, there is a critical lack of data on the mechanical behavior of alloys of interest for MSRS such as 316H, 617 and 709 in molten fluoride (FLiNaK or FLiBe) or chloride (NaCl-$MgCl_2$) salts. Limited legacy data from the molten salt reactor experiment (MSRE) program [7] showed a significant reduction in creep rupture strength of a Ni-base alloy (Ni-15Cr-7Fe wt.%) in the molten fluoride NaF-ZrF4-UF4 (50-46-4 mol.%) salt. With ongoing efforts to commercialize different molten salt reactor concepts, the industry can considerably benefit from quantitative information on the impact of molten halide salts on the engineering properties such as creep and fatigue strength of materials of interest.

Creep tests for 316H were conducted with fluoride (FLiNaK) and chloride (NaCl-$MgCl_2$) salts tat 650°C/150 MPa while alloys 709 and 617 were tested with FLiNaK at 700C/158 MPa and 750C.146 MPa respectively. Baseline tests were conducted in air to assess the impact of the molten salts on the creep behavior.

Procedure

The cylindrical hollow creep specimens had a 57.2 mm gage length, 12.7 mm outer and 11.2 mm inner diameter (ID). A stainless-steel cup made of type 316L stainless steel was attached to the bottom of the creep specimen to capture the molten salt after rupture. This specimen design was derived from a patent application [8]. All specimens were subjected to rigorous geometry checks in order to verify dimensions and surface finish. Particularly, the inner surface was electrical discharge machined (EDM) and polished to an Ra of 0.4 µm measured using a profilometer.

Table 1: Compositions of the studied alloys in wt.% determined by plasma/combustion analyses

Alloy	Fe	Cr	Ni	Mn	Si	Mo	C	Co	Al	Ti	Other
316H	Bal.	16.6	10.3	1.6	0.3	2.0	0.04	0.2	-	-	Cu 0.4 N 0.03
709	Bal.	20.0	24.6	0.9	0.35	1.5	0.08	-	-	-	Nb 0.2
617	1.6	22.2	Bal.	0.1	0.1	8.6	0.05	11.6	1.1	0.4	Cu 0.04
282	0.8	19.4	Bal.	-	-	8.5	0.06	10.2	1.5	2.2	Zr 0.01

Specimens of 316H were machined from a 2.54 cm thick 316H plate provided in a solution annealed state. The creep specimens of alloy 709 were machined from a 4.6 cm plate produced by ATI Flat Rolled Products. The as-received plate was solution annealed at a minimum temperature of 1150°C followed by a precipitation treatment at 775°C for 10h. Alloy 617 specimens were machined from a 3.7 cm thick solution annealed plate provided by Thyssen Krupp VDM with an average grain size of 150 µm. The measured composition of the three alloys is given in Table 1.

The FLiNaK salt used for this work was prepared by a now defunct company Electrochemical Systems. The composition of the as-received salt was previously reported [6] . The NaCl–$MgCl_2$ eutectic salt used in this study was prepared with 58.5 mol% anhydrous NaCl salt and 41.5 mol% anhydrous $MgCl_2$ salt. The salt was homogenously mixed and purified following an established purification procedure for chloride salts [9]. The trace impurities of the NaCl–$MgCl_2$ eutectic salt mixture were identified by inductively coupled plasma mass spectrometry (ICP-MS) analysis [10] in which the most prominent impurity elements and the corresponding concentrations were 0.79 ppm Li, 5.44 ppm S, 15.7 ppm K, 6.99 ppm Ca, 0.03 ppm Cr, 0.01 ppm Mn, 0.13 ppm Fe, 0.23 ppm Ni (weight). The oxygen level in the salt was ~300-400 wppm.

The hollow creep specimens were filled in an Ar-filled glovebox (O_2 and H_2O < 0.1 ppm) with ~15 g of the salt and sealed by welding the cap (same material as the specimen) on the top in the glovebox. Before beginning the creep test, thermocouples were fixed at about 1/3 of the gauge length before threading on the catch cup. The completed load train (including the pull rods and specimen) was loaded into the furnace and threaded into the turn buckle before additional insulation was applied. The heating was 1 h to temperature followed by a 0.5 h hold to reach a steady state. The system was operated within a 3°C variance between the thermocouple on the specimen and the control thermocouple of the furnace. The linear variable displacement transducer (LVDT) used to measure displacement and derive creep strains was zeroed at this point and the specimen was loaded. The furnace was programmed to be switched off immediately upon specimen rupture to minimize corrosion damage to the specimen due to the leaking molten salt. The test matrix for the creep tests is given in Table 1.

Table 1. Test matrix for the creep tests

Alloy	**Temperature (°C)**	**Stress (MPa)**	**Environment**
316H	650	150	Air
			FLiNaK
			NaCl-$MgCl_2$
709	700	158	Air
			FLiNaK
617	750	146	Air
			FLiNaK

Post-exposure, specimens were cross-sectioned for metallographic analyses. The mounted samples were ground to 1200 grit with SiC grinding papers and subsequently polished with diamond pastes to 1 μm surface finish. Microstructural characterization to measure compositional changes and identify phase transformations was performed using scanning electron (SE), back-scattered electron (BSE) microscopy (TESCAN MIRA3 SEM) and energy dispersive x-ray spectroscopy (EDS:EDAX Octane Elect Super Silicon Drift Detector).

Results

Figure 1 shows the measured creep strains of 316H in air, FLiNaK and NaCl-$MgCl_2$ at 650 °C/150 MPa. The molten salt environment has evidently reduced the creep rupture life of the alloy in FLiNaK compared to the baseline creep rupture lifetime in air (~50% reduction from 1702h to 793h). Additionally, there is evidently a significant reduction in creep ductility due to the molten salt environment. However, the test with NaCl-$MgCl_2$ did not affect the creep rupture lifetime with the specimen failing after 1948h. This is a surprising result since an earlier test at 650°C/160 MPa had shown a ~30% reduction in creep rupture lifetime compared to the exposure in air [11]. An additional creep test with NaCl-$MgCl_2$ was started to repeat this condition and verify reproducibility.

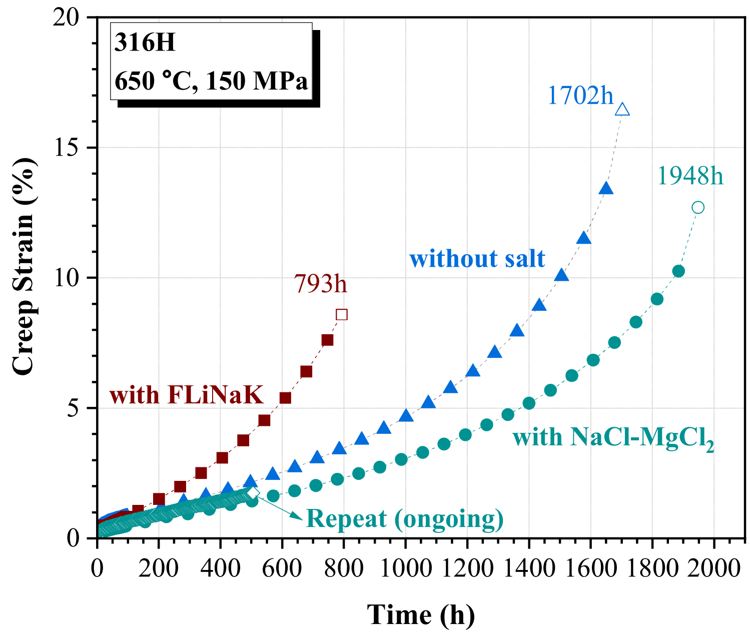

Figure 1: Measured creep strains of 316H in air, FLiNaK, NaCl-$MgCl_2$ at 650°C/150 MPa. Open symbols indicate failure time.

The creep behavior of 709 was significantly affected by the molten salt environment (Figure 2). The specimen tested with FLiNaK failed after 150h compared to the 1095h creep rupture time for the specimen tested in air. The test with FLiNaK was repeated and the specimen failed after 273h with a creep strain of 1.3% suggesting a brittle fracture.

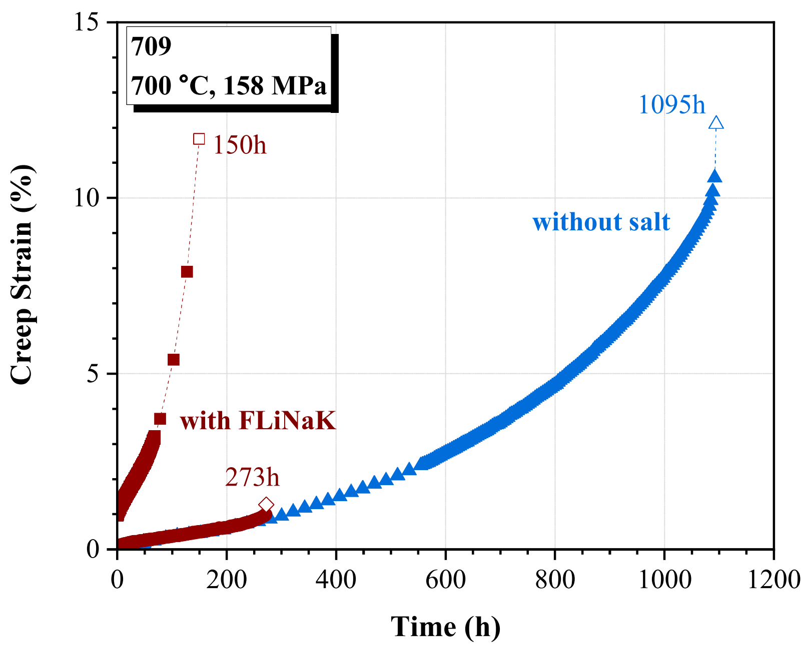

Figure 2: Measured creep strains of 709 in air and FLiNaK at 700°C/158 MPa. Open symbols indicate failure time.

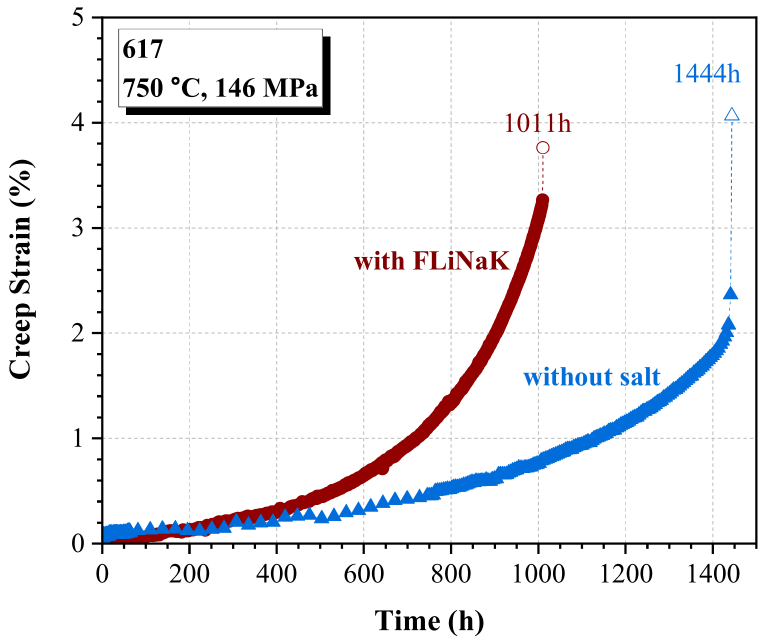

Figure 3: Measured creep strains of 617 in air and FLiNaK at 750°C/146 MPa. Open symbols indicate failure time.

Figure 3 shows the measured creep strains of 617 in air and FLiNaK at 750 °C and 146 MPa. The creep strains were relatively low for both 617 specimens compared to the data for 617 in the literature [12]. This might be due to the lower number of grains expected across the wall thickness of the current specimen geometry (0.76 mm) which is below the recommended wall thickness of 3.175 mm [12]. The specimen tested in FLiNaK showed about a 30% reduction in creep rupture time.

Conclusions

The creep tests with FLiNaK resulted in the reduction of creep rupture lifetime of all investigated alloys with the impact being the strongest on alloy 709. For 316H, the test with NaCl-$MgCl_2$ did not influence creep rupture lifetime at 650°C/150 MPa but was observed to reduce creep rupture lifetime at 650°C/160 MPa in an earlier work. The ongoing repeat test will provide additional data and aid in confirming the observation. The assessment of the impact of molten fluoride and chloride salts on creep behavior of 316H, 709 and 617 at different stresses will be continued in FY25. There is an additional focus on identifying the precise mechanisms of creep-corrosion interactions to provide insights into the observed creep rupture data.

References

1. Locatelli, G., M. Mancini, and N. Todeschini, *Generation IV nuclear reactors: Current status and future prospects.* Energy Policy, 2013. **61**: p. 1503-1520.
2. Serp, J., et al., *The molten salt reactor (MSR) in generation IV: Overview and perspectives.* 2014. **77**: p. 308–319.
3. Zhao, H., et al., *Development, Verification, and Validation of an Advanced Systems Code KP-SAM for Kairos Power Fluoride Salt–Cooled High-Temperature Reactor (KP-FHR).* Nuclear Science and Engineering, 2023. **197**(5): p. 813-839.

4. Kelleher, B.C., S.F. Gagnon, and I.G. Mitchell, *Thermal gradient mass transport corrosion in NaCl-MgCl2 and MgCl2-NaCl-KCl molten salts.* Materials Today Communications, 2022. **33**: p. 104358.
5. Macpherson, H.G., *Development of Materials and Systems for Molten-Salt Reactor Concept.* Reactor Technology, 1972. **15**(2): p. 136-155.
6. Raiman, S.S., et al., *Corrosion of 316H stainless steel in flowing FLiNaK salt.* Journal of Nuclear Materials, 2022. **561**: p. 153551.
7. Manly, W.D., et al., *AIRCRAFT REACTOR EXPERIMENT--METALLURGICAL ASPECTS*. 1958, ORNL-2349 United States 10.2172/4227617 NTIS ORNL ; Oak Ridge National Lab., Tenn. p. 57.
8. Ren, W. Molten salt environment creep testing extensometry system U.P. Office 10895519 B2 UT - Battelle , LLC , Oak Ridge , TN 2021
9. Mayes, R.T., et al., *Purification of Chloride Salts for Concentrated Solar Applications*. 2018, ORNL/LTR-2018/1052, ORNL: United States.
10. Wang, Y., et al., *Radionuclide tracing based in situ corrosion and mass transport monitoring of 316L stainless steel in a molten salt closed loop.* Nature Communications, 2024. **15**(1): p. 3106.
11. Pillai, R.P.B.A. *Assessing the impact of molten halide salts on creep of structural alloys at 650°-750°C*. in *10th International Conference on Advances in Materials, Manufacturing & Repair for Power Plants*. 2024. Bonita Springs, FLORIDA: ASM International.
12. Wright, R.N., *Draft ASME Boiler and Pressure Vessel Code Cases and Technical Bases for Use of Alloy 617 for Constructions of Nuclear Component Under Section III, Division 5*. 2021: United States.